Energy harvesting via wrinkling instabilities

Ashkan Haji Hosseinloo and Konstantin Turitsyn

Citation: Appl. Phys. Lett. **110**, 013901 (2017); doi: 10.1063/1.4973524
View online: http://dx.doi.org/10.1063/1.4973524
View Table of Contents: http://aip.scitation.org/toc/apl/110/1
Published by the American Institute of Physics

Energy harvesting via wrinkling instabilities

Ashkan Haji Hosseinloo[a] and Konstantin Turitsyn[b]
Department of Mechanical Engineering, Massachusetts Institute of Technology 77 Massachusetts Avenue, Cambridge, Massachusetts 02139, USA

(Received 27 September 2016; accepted 20 December 2016; published online 3 January 2017)

Conventional vibratory energy harvesters, working based on linear resonance, suffer from narrow bandwidth and are very inefficient at small scale for low frequency harvesting. Here, to improve the harvesting effectiveness, we propose to exploit surface instability or in general instability in layered composites where intriguing morphological patterns with large strain are formed under compressive loads. The induced large strains, which are independent of the excitation frequency, could be exploited to give rise to large strains in an attached piezoelectric layer to generate charge and, hence, energy. In this study, we particularly focus on wrinkling of a stiff interfacial layer embedded within a soft matrix. We derive the governing dynamical equation of thin piezoelectric patches attached at the peaks and troughs of the wrinkles. Results show that wrinkling could help to increase the harvested power by more than an order of magnitude. *Published by AIP Publishing.* [http://dx.doi.org/10.1063/1.4973524]

Advances in electronics in the last decade have brought about sea-change shift towards miniaturized low-power electronic devices. The significant reduction in electronics energy consumption has made energy harvesting from ambient vibration, a universal and abundant source of energy, a viable alternative to the bulky and costly traditional batteries.[15,16] A conventional vibratory energy harvester (VEH) consists of a vibratory host with an attached transduction mechanism which is usually based on piezoelectric,[8,10,29] electromagnetic,[1] or electrostatic effect.[24] Conventional VEHs operate based on linear resonance which suffer from narrow-band harvesting spectrum. Furthermore, they are extremely inefficient at small scale for low-frequency harvesting as it is either hard to realize the low-frequency resonance at small scale, or the natural frequency of the VEH is bounded from below by an imposed displacement limit.[13]

To overcome the aforementioned narrow bandwidth, purposeful inclusion of nonlinearity has been the focus of the majority of the studies in the field over the last few years.[7] Multi-stable harvesters including penta-,[19] tri-,[3,28,34] and in particular, bi-stable[5,9,12,14,27] VEHs have been investigated so as to widen the harvesting bandwidth. Two other classes of the nonlinear harvesters have been proposed to enhance the harvesting efficacy, mainly at the low excitation frequencies, namely, the up-conversion technique[17,21,32] and the buy-low-sell-high (BLSH) strategy which maximizes the energy flow to the system.[13,14] Although all these techniques have improved the harvesting process, they have their own drawbacks including lack of robustness to the system or excitation parameters, being unable to address the two issues of narrow bandwidth and low-frequency harvesting at the same time, or being difficult to implement at the small scale.

In this letter, we propose to exploit instabilities in multi-layered composites or surface instabilities. Although the structure of the systems in which these two classes of instabilities occur are different, the underlying cause and basis are quite the same: a stiff film/layer surrounded from one or two sides by a thicker and softer material. When a stiff layer sitting on a soft foundation or embedded in a soft matrix is subjected to compressive stress, it may go unstable with different instability patterns. The induced instability results in high local strains that could be exploited for energy harvesting which is the focus of this letter. The large local strain is the result of two mechanisms: (i) When the stiff layers go unstable, they take almost no more load resulting in lower composite stiffness. This consequently leads to large macroscopic strain when the instability occurs. (ii) The nonlinear geometric pattern of the stiff layer (e.g., sinusoid in wrinkling) locally amplifies the macroscopic strain. A key advantage of these types of instabilities is that they are independent of the excitation (compressive force) frequency.

Intriguing morphologies and surface patterns in nature at different scales from wrinkles on skins of mammalians, plants, and fruits[4,20,33] to crumpled membranes of blood cells[30] have inspired a big body of research in soft matter instabilities. Recent studies in this field have found applications in other disciplines including soft lithography, metrology, flexible electronics, and biomedical engineering.[22] Here, we extend the application of soft matter instabilities to kinetic energy harvesting.

Surface instabilities are grouped into five main categories: wrinkle, crease, fold, period-double,[26] and ridge.[31] Based on the phase diagram developed by Wang and Zhao,[31] wrinkling is the most common surface instability if there is no delamination in the layers; hence, we focus on the wrinkling instability in this study. Based on the classic beam theory, a clamped beam buckles under axial compressive force in its first mode (with a mode shape similar to a half sine) before any other modes take place. In fact, other modes never take place because they posses larger potential energy than the first mode. However, if the beam is sitting on a softer elastic foundation or embedded in an elastic softer matrix, the beam buckles in higher modes which are usually

[a]Electronic mail: ashkanhh@mit.edu
[b]Electronic mail: turitsyn@mit.edu

referred to as wrinkling. The unconventional higher mode buckling occurs simply because the system always seeks a configuration with the lowest potential energy; and above a critical stiffness of the foundation/matrix, the higher modes of buckling posses lower potential energy than the classic half-wavelength buckling mode.

Figure 1 illustrates schematically how energy is harvested via wrinkling instability. Piezoelectric patches are attached at two sides of the interfacial layers at the peaks and troughs of the wrinkles. Here, we assume the coupling between the piezoelectric patches and the interfacial layer is weak, and hence, the piezoelectric effect on the wrinkling phenomenon is negligible; in other words, there is one-way feedback from the wrinkling to the piezoelectric layer. This allows us to study the wrinkling mechanics independent of the piezoelectric layer and then feed the interfacial layer response as the input to the piezoelectric layer. We also assume a plane strain condition. The strains at any point along the interfacial layer are given by[18]

$$\begin{aligned}
&\varepsilon_1(x,z,\bar{\varepsilon}) = \bar{\varepsilon}_{\mathrm{cr}} + \frac{4\pi z}{\lambda(\bar{\varepsilon})}\sqrt{|\bar{\varepsilon}| - |\bar{\varepsilon}_{\mathrm{cr}}|}\,\sin\left(\frac{2\pi x}{\lambda(\bar{\varepsilon})}\right),\\
&\varepsilon_3(x,z,\bar{\varepsilon}) = -\frac{\nu_f}{1-\nu_f}\varepsilon_1(x,z,\bar{\varepsilon}),\\
&\varepsilon_{13}(x,z,\bar{\varepsilon}) \approx 0, \quad \varepsilon_2(x,z,\bar{\varepsilon}) = \varepsilon_{12}(x,z,\bar{\varepsilon}) = \varepsilon_{23}(x,z,\bar{\varepsilon}) = 0.
\end{aligned} \tag{1}$$

In Eq. (1), $\bar{\varepsilon}_{\mathrm{cr}}$ is the critical macroscopic strain at which wrinkling starts, and $\bar{\varepsilon}$ is the applied macroscopic post-buckling strain. $\lambda(\bar{\varepsilon})$ is wavelength of the wrinkle and z is the distance from the neutral axis of the interfacial layer/film. The Poisson ratio of the interfacial layer is denoted by ν_f. Assuming the overall contour length of the interface is preserved, the kinematics enforce that $\lambda(\bar{\varepsilon}) = \lambda_{\mathrm{cr}} e^{-|\bar{\varepsilon}|}$ with λ_{cr} being the initial wrinkle wavelength.[18] The critical macroscopic strain $\bar{\varepsilon}_{\mathrm{cr}}$ and the initial wrinkling wavelength λ_{cr} are given by[2,23]

$$\begin{aligned}
\bar{\varepsilon}_{\mathrm{cr}} &= -3^{\frac{2}{3}}\left(\frac{3-4\nu_m}{(1-\nu_m)^2}\right)^{\frac{-2}{3}}\left(\frac{E_f}{E_m}\right)^{-\frac{2}{3}},\\
\lambda_{\mathrm{cr}} &= \pi t\left(\frac{1}{3}\right)^{\frac{1}{3}}\left(\frac{3-4\nu_m}{(1-\nu_m)^2}\right)^{\frac{1}{3}}\left(\frac{E_f}{E_m}\right)^{\frac{1}{3}},
\end{aligned} \tag{2}$$

where ν_m is the Poisson ratio of the matrix, and E_f and E_m are Young's moduli of the interfacial layer and the matrix, respectively. Thickness of the interfacial layer is designated by t. As mentioned earlier, the advantage of exploiting instability for increased local strain is twofold: first, just based on kinematics, the nonlinear instability pattern, e.g., Eq. (1) in this study, induces larger strain than the macroscopic strain; however, more importantly, the macroscopic strain is greatly amplified as a result of the instability. This is due to the fact that once the interfacial layer buckles it takes no more load which consequently results in decreased overall stiffness of the composite. The macroscopic strain $\bar{\varepsilon}$ could be mathematically formulated as

$$\bar{\varepsilon}(t) = \begin{cases} \dfrac{\bar{\sigma}(t)}{E^i_{\mathrm{comp}}}; & |\bar{\sigma}(t)| < |\bar{\sigma}_{\mathrm{cr}}| \\ \bar{\varepsilon}_{\mathrm{cr}} + \dfrac{(\bar{\sigma}(t) - \bar{\sigma}_{\mathrm{cr}})}{E^f_{\mathrm{comp}}}; & |\bar{\sigma}(t)| \geq |\bar{\sigma}_{\mathrm{cr}}|, \end{cases} \tag{3}$$

where $\bar{\sigma}_{\mathrm{cr}} = E^i_{\mathrm{comp}}\bar{\varepsilon}_{\mathrm{cr}}$ is the critical stress at the onset of the wrinkling. E^i_{comp} and E^f_{comp} denote the effective plane-strain Young's modulus of the composite before and after the wrinkling instability, respectively. Effective Young's modulus of the composite before wrinkling could be calculated as $E^i_{\mathrm{comp}} = \eta_m \bar{E}_m + \eta_f \bar{E}_f$, where η_m and η_f represent volumetric ratios of the matrix and the interfacial layer, respectively. Also, $\bar{E}_m = E_m/(1-\nu_m^2)$ and $\bar{E}_f = E_f/(1-\nu_f^2)$ define the plane-strain Young's moduli of the matrix and the interfacial layer, respectively. Once the interfacial layers wrinkle, the effective stiffness of the composite drops with a good approximation to $E^f_{\mathrm{comp}} = \eta_m \bar{E}_m$.

Having the full description of the strain states in the interfacial layers which are assumed to be the same as those in the piezoelectric layer, we look into the piezoelectric layer. Polarization direction of the piezo layer is placed along the $3(z)$ axis. For plane strain deformation ($\varepsilon_2 = 0$), the strains and the electrical field E_3 along the polarization direction $3(z)$ satisfy the constitutive relation[6,11,25] $D_3 = k^s_{33}E_3 + e_{31}\varepsilon_1 + e_{33}\varepsilon_3$, where the electric displacement D_3 is to be found. e_{ij} and k_{ij} are the piezoelectric and the dielectric constants, respectively. In view of Eq. (1), ε_3 could be replaced in the piezoelectric constitutive relation, and hence, it could be simplified as

$$D_3 = k^s_{33}E_3 + \left(e_{31} - \frac{\nu_f}{1-\nu_f}e_{33}\right)\varepsilon_1 = k^s_{33}E_3 + \bar{e}\varepsilon_1. \tag{4}$$

The current running through a piezoelectric layer is calculated by time-differentiating the integral of the electric displacement over the piezo surface as $i = \frac{d}{dt}\int_{A_p} D_3 dA = A_p \dot{D}_3$, where overdot denotes differentiation with respect to time. The last expression is derived assuming that the length of the piezo patch is small enough so that D_3 is constant over the length of the piezo layer. A_p is the total area of each piezo layer. We now consider a case where N of the piezo patches are connected in series to an external resistive load characterised by the resistance R. Let us also assume that the electric field E_3 across the thickness of each piezo layer is constant; hence, the voltage across each layer equals $t_p E_3$ with t_p being the piezo layer thickness. Then equating the current running through the resistive load and the piezoelectric layers and substituting D_3 from Eq. (4), the governing dynamic equation is derived as

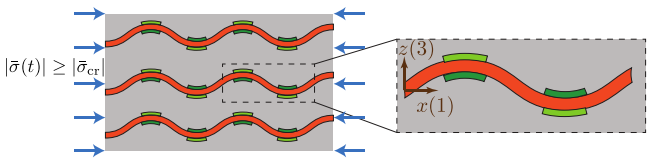

FIG. 1. Energy harvesting via wrinkling phenomenon. The figure on the left shows a representative element of a soft matrix containing three stiff interfacial layers/films with piezoelectric patches attached on two sides of the films at the peaks and troughs. The figure on the right depicts larger view of a segment (one wavelength) of the interfacial layer with attached coordinate system where direction x or 1 and z or 3 are aligned with and perpendicular to the interfacial layer, respectively. Wiring and electrical interconnections could be mainly embedded within the soft matrix and the harvesting itself could take place outside the whole structure.

$$\dot{v} + \left(\frac{Nt_p}{k_{33}^s A_p R}\right) v = -\frac{Nt_p \bar{e}}{k_{33}^s} \dot{\varepsilon}_1. \tag{5}$$

Equation (5) is a first order differential equation that could be solved both analytically and numerically given the input $\dot{\varepsilon}_1$. ε_1 is equal to the macroscopic strain before buckling, but will follow Eq. (1) once the buckling takes place. Assuming that the piezo patches are small in length and are placed at the peaks and troughs, we can approximate $\sin(\frac{2\pi x}{\lambda(\bar{\varepsilon})}) \approx 1$ in Eq. (1), and hence the excitation strain rate $\dot{\varepsilon}_1$ in the interfacial and the piezo layers will take the form

$$\dot{\varepsilon}_1(t) = \begin{cases} \dot{\bar{\varepsilon}}(t); & |\bar{\varepsilon}(t)| < |\bar{\varepsilon}_{cr}| \\ -\frac{4\pi z}{\lambda_{cr}} \left(\frac{|\bar{\varepsilon}(t)| - |\bar{\varepsilon}_{cr}| + 0.5}{\sqrt{|\bar{\varepsilon}(t)| - |\bar{\varepsilon}_{cr}|}} \right) \text{sign}(\bar{\varepsilon}(t)) e^{|\bar{\varepsilon}(t)|} \dot{\bar{\varepsilon}}(t); & \text{else.} \end{cases} \tag{6}$$

The material properties and the geometric dimensions of the matrix, interfacial layer, and the piezoelectric patches are given in Table I. b_p in this table denotes the depth of the piezoelectric patches. The length of the piezoelectric patches l_p is set to one sixth of the initial wrinkling wavelength, i.e., $l_p = 1/6\lambda_{cr}$. For the parameters in Table I, the critical macroscopic strain $\bar{\varepsilon}_{cr}$, and the initial wavelength λ_{cr} are equal to -0.0384 and 0.8027 mm, respectively.

In this study, we consider a slowly varying sine-squared compressive macroscopic stress $\bar{\sigma}(t) = -\bar{\sigma}_{amp} \sin^2(0.5\omega t)$ with amplitude $\bar{\sigma}_{amp} = 30$ MPa, and frequency $\omega = 2\pi(0.5)$ rad/s. Figure 2 shows the induced macroscopic strain and the local strain along the interfacial layer ε_1 for $z = -t/2$ in Eq. (1). It could be seen that when the critical strain ($\bar{\varepsilon}_{cr} = -0.0384$) is exceeded, wrinkling takes place and both the magnitude and the rate of the induced strain in the interfacial layer are increased.

To have a fair comparison between two cases of harvesting with and without the wrinkling phenomenon, we first optimize the average harvested power with respect to the external load. The average harvested power is defined as the time-average of the dissipated power in the external load: $P_{ave} = \frac{1}{T}\int_0^T \frac{v(t)^2}{R} dt$ for a large value of T. The optimal resistive loads are found to be $2.0 \times 10^{11}\,\Omega$, and $2.5 \times 10^{11}\,\Omega$ for the cases with and without the wrinkling, respectively. These optimal loads are used for the rest of the simulations.

TABLE I. Material properties and geometric dimensions of the matrix, interfacial layer, and the piezoelectric patches.

Parameter	Value
E_m	50 MPa
E_f	5 GPa
ν_m	0.48
ν_f	0.48
T	50 μm
t_p	1 μm
η_f	0.0625
b_p	0.1 mm
e_{31}	-0.3041 C/m^2
e_{33}	-0.4865 C/m^2
k_{33}^s	0.106×10^{-9} C/Vm
N	1

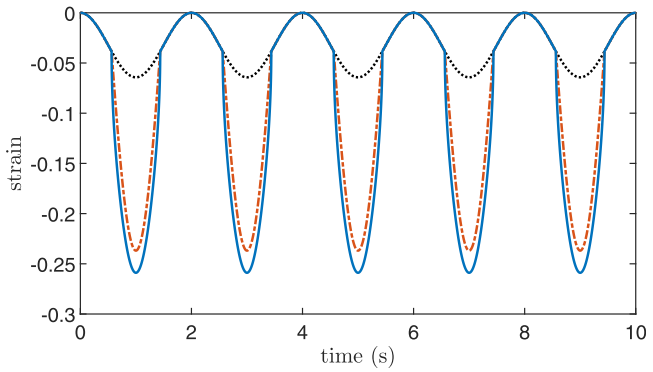

FIG. 2. Time history of the induced macroscopic strain $\bar{\varepsilon}(t)$ and the local strain in and along the interfacial layer $\varepsilon_1(t)$. The black dotted line shows the macroscopic and the interfacial layer strain if there was no wrinkling phenomenon. The red dashed-dotted and the blue solid lines represent the macroscopic strain in the composite and the local strain in the interfacial layer in the presence of the wrinkling, respectively.

As a result of the increased induced strain and its time rate, the external load is excited by a larger current source, and hence, the voltage induced at the external load is increased. Consequently, the energy harvesting is dramatically improved. Figure 3 shows the time histories of the induced voltage and the harvested energy. Based on the figure, the induced voltage is increased, and subsequently, the harvested energy is improved by about 20 times. It should be noted that if the whole volume is made of the piezoelectric material (assumed to have large stiffness), a comparable level of energy could be harvested even though no instability takes place and it compresses uniformly, but at the cost of a much stiffer system which in many applications is not acceptable.

Assuming zero initial conditions for the voltage v, the solution to Eq. (5) could be written as $v(t) = -\frac{Nt_p \bar{e}}{k_{33}^s} e^{-\frac{Nt_p}{k_{33}^s A_p R} t} \int_0^t \dot{\varepsilon}_1(t) e^{\frac{Nt_p}{k_{33}^s A_p R} t} dt$. Now if $e^{\frac{Nt_p}{k_{33}^s A_p R} t}$ is bounded from above, the whole expression is bounded even though $\dot{\varepsilon}_1(t)$ momentarily goes to infinity at the onset of the wrinkling, i.e., $|\bar{\varepsilon}| = |\bar{\varepsilon}_{cr}|$. It could also be noticed that if $\frac{Nt_p}{k_{33}^s A_p R} \ll 1$, the induced voltage $v(t)$ is proportional to the induced strain $\varepsilon_1(t)$. For the parameters used for the simulations in this study, $\frac{Nt_p}{k_{33}^s A_p R}$ is not

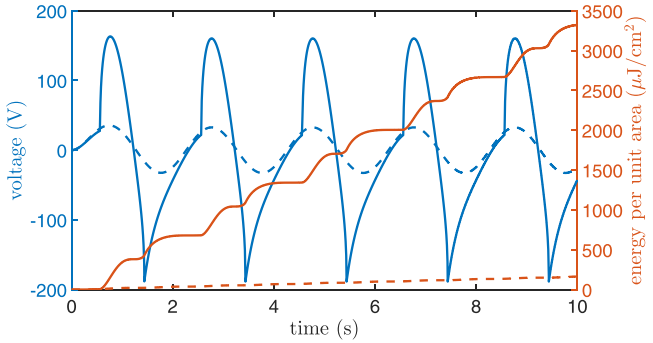

FIG. 3. Time history of the induced voltage $v(t)$, and the average harvested power across the external load with (solid line) and without (dashed line) the wrinkling phenomenon.

too small (it is about 3.5) so the voltage response is more involved than just being proportional to the strain.

There is another subtle reason to the improved harvesting performance in addition to the large induced strains: wrinkling helps the system to passively mimic the BLSH strategy[13] proven by the authors' earlier work to maximize the energy flow into the system. Typical soft matter instabilities occur after a critical applied stress/strain is exceeded. This means the system is not experiencing a large displacement/deformation until a larger value of the excitation force is reached. The larger displacement as a result of the instability, at a large input force simply means larger flow of energy to the system.

In conclusion, we proposed to exploit soft matter instabilities to improve energy harvesting, and theoretically investigated this idea for wrinkling instabilities as the most common instability in the soft matter. The idea lies in the suddenly induced large strains in this class of instabilities mainly due to the effective softening behaviour, and the large-strain nonlinear instability patterns. Both the large magnitude and the time rate of thus induced strains could subsequently induce large charge and current in a piezoelectric patch locally attached in the vicinity of the high strains. A big advantage of harvesting via such instabilities is that they are independent of excitation frequency. Theoretical and simulation results show that wrinkling could help to increase the harvested power by more than an order of magnitude. We believe the proposed approach opens the way to previously uncharted energy harvesting paradigms, and in view of the recent advances in flexible electronics,[6] introduces a promising method to effectively harvest energy for a wide range of applications.

[1]B. Alavikia, T. S. Almoneef, and O. M. Ramahi, Appl. Phys. Lett. **104**, 163903 (2014).
[2]H. G. Allen, *Analysis and Design of Structural Sandwich Panels*, Commonwealth and International Library. Structures and Solid Body Mechanics Division (Pergamon Press, Oxford; New York, 1969).
[3]J. Cao, S. Zhou, W. Wang, and J. Lin, Appl. Phys. Lett. **106**, 173903 (2015).
[4]E. Cerda and L. Mahadevan, Phys. Rev. Lett. **90**, 074302 (2003).
[5]F. Cottone, H. Vocca, and L. Gammaitoni, Phys. Rev. Lett. **102**, 080601 (2009).
[6]C. Dagdeviren, B. D. Yang, Y. Su, P. L. Tran, P. Joe, E. Anderson,J. Xia, V. Doraiswamy, B. Dehdashti, X. Feng, *et al.*, Proc. Natl. Acad. Sci. **111**, 1927 (2014).
[7]M. F. Daqaq, R. Masana, A. Erturk, and D. D. Quinn, Appl. Mech. Rev. **66**, 040801 (2014).
[8]A. Erturk, O. Bilgen, and D. Inman, Appl. Phys. Lett. **93**, 224102 (2008).
[9]A. Erturk, J. Hoffmann, and D. Inman, Appl. Phys. Lett. **94**, 254102 (2009).
[10]A. Erturk and D. J. Inman, Smart Mater. Struct. **18**, 025009 (2009).
[11]X. Feng, B. D. Yang, Y. Liu, Y. Wang, C. Dagdeviren, Z. Liu, A. Carlson, J. Li, Y. Huang, and J. A. Rogers, ACS Nano **5**, 3326 (2011).
[12]L. Gammaitoni, I. Neri, and H. Vocca, Appl. Phys. Lett. **94**, 164102 (2009).
[13]A. H. Hosseinloo and K. Turitsyn, Phys. Rev. Appl. **4**, 064009 (2015).
[14]A. H. Hosseinloo and K. Turitsyn, Smart Mater. Struct. **25**, 015010 (2016).
[15]A. H. Hosseinloo and K. Turitsyn, Smart Mater. Struct. **25**, 055023 (2016).
[16]A. H. Hosseinloo and K. Turitsyn, Proc. SPIE **9799**, 97991L (2016).
[17]S.-M. Jung and K.-S. Yun, Appl. Phys. Lett. **96**, 111906 (2010).
[18]N. Kaynia, "Instability-induced transformation of interfacial layers in composites and its multifunctional applications," Ph.D. thesis (Massachusetts Institute of Technology, 2016).
[19]P. Kim and J. Seok, J. Sound Vib. **333**, 5525 (2014).
[20]M. Kücken and A. C. Newell, Europhys. Lett. **68**, 141 (2004).
[21]H. Kulah and K. Najafi, IEEE Sens. J. **8**, 261 (2008).
[22]B. Li, Y.-P. Cao, X.-Q. Feng, and H. Gao, Soft Matter **8**, 5728 (2012).
[23]Y. Li, N. Kaynia, S. Rudykh, and M. C. Boyce, Adv. Eng. Mater. **15**, 921 (2013).
[24]Y. Lu, F. Cottone, S. Boisseau, F. Marty, D. Galayko, and P. Basset, Appl. Phys. Lett. **107**, 253902 (2015).
[25]A. Meitzler, H. Tiersten, A. Warner, D. Berlincourt, G. Couqin, and F. Welsh III, in IEEE Standard on Piezoelectricity (1988).
[26]Sometimes period-double or even period-quadruple are categorized under wrinkling, e.g., in Ref. 22.
[27]S. C. Stanton, C. C. McGehee, and B. P. Mann, Phys. D **239**, 640 (2010).
[28]G. O. Tékam, C. K. Kwuimy, and P. Woafo, Chaos: Interdiscip. J. Nonlinear Sci. **25**, 013112 (2015).
[29]A. Toprak and O. Tigli, Appl. Phys. Rev. **1**, 031104 (2014).
[30]L. Wang, C. E. Castro, and M. C. Boyce, Soft Matter **7**, 11319 (2011).
[31]Q. Wang and X. Zhao, Sci. Rep. **5**, 8887 (2015).
[32]A. Wickenheiser and E. Garcia, Smart Mater. Struct. **19**, 065020 (2010).
[33]J. Yin, Z. Cao, C. Li, I. Sheinman, and X. Chen, Proc. Natl. Acad. Sci. **105**, 19132 (2008).
[34]S. Zhou, J. Cao, J. Lin, and Z. Wang, Eur. Phys. J. Appl. Phys. **67**, 30902 (2014).